Revision of Quasi-chemical Viscosity Model for Viscosity Estimation of Molten Multi-component Oxide Slag

Masanori SUZUKI [1)] and Evgueni JAK [2)]

1) -now, Graduate School of Engineering, Osaka University, 2-1 Yamadaoka, Suita, 565-0871 Osaka, Japan, 2)-former.

2) Pyrometallurgy Research Centre, The University of Queensland, St Lucia, Brisbane, QLD 4072 Australia

Abstract: A quasi-chemical viscosity model (QCV) had been previously developed that enables the viscosities of multi-component molten oxide slags to be predicted within experimental uncertainties over wide ranges of composition and temperature. The Eyring equation is used to express viscosity as a function of composition and temperature. The QCV model links the vaporisation and activation energies to the slag internal structure through the concentrations of various $Si_{0.5}O$, $Me^{n+}_{2/n}O$ and $Me^{n+}_{1/n}Si_{0.25}O$ viscous flow structural units. The concentrations of these structural units are derived from a quasi-chemical thermodynamic model of the liquid slag. In the present study, the quasi-chemical viscosity model formalism has been revised, and a number of shortcomings in the previous model have been resolved. The links between model parameters and fundamental physical properties or structural characteristics of oxide melts have been introduced with reference to physical basis of the model. Agreement with the available experimental viscosity data has been improved. The QCV model parameters have been successfully extended to the multi-component SiO_2 - Al_2O_3 - CaO - MgO - Na_2O - K_2O - 'FeO' - Fe_2O_3 - PbO - ZnO system, and over 7000 experimental viscosity data in this system have been reproduced within 25 % as the average of the relative errors.

Key words: Viscosity, Model, Multi-component oxide systems, Viscous flow structural unit

1. Introduction

Slag viscosity is a key property essential for a number of metallurgical and power generation industrial processes. The authors have focused on the development of a reliable and general viscosity model for complex slag systems. In the present study, the formalism of a structurally-based quasi-chemical viscosity model [1-7] has been revised in for the application to fully liquid slags of multi-component oxide systems. Similar to other structurally-based viscosity slag models [8-12], the link between viscosities and the complex internal slag structure at atomic level improves predictive capability of slag viscosities.

2. Model Description

Frenkel's kinetic theory [12] considers a liquid to possess a solid-like structure with molecules, or more generally, structural units (SU), oscillating in their energetic cells (potential wells) near average positions. Oscillations higher in magnitude than the potential barrier result in the movement of a structural unit into an adjacent vacant cell, or "hole", provided the latter is vacant. These vacant cells, or "holes", formed in the liquid as a result of fluctuations, are distributed randomly throughout the liquid. Therefore, the viscosity of liquid as a reaction to the applied shear force is determined by (i) the ability of a structural unit to jump over the potential barrier and (ii) the presence of "holes" in the liquid. The following Eyring viscosity Equation (1) was derived [13] using the above principles:

$$\eta = \frac{2RT}{\Delta E_V} \frac{(2\pi m_{SU} kT)^{1/2}}{v_{SU}^{2/3}} \exp\left(\frac{E_a}{RT}\right) \quad (\eta \text{ in Pa*s}) \tag{1}$$

where R [J/K/mol] and k [J/K] are the gas and the Boltzmann constants, $\pi \approx 3.1416$, T is the absolute temperature [K], m_{SU} [kg] and v_{SU} [m^3] are the average mass and volume of viscous flow structural units. The activation energy E_a reflects the interactions between different structural units in the liquid. The energy of vaporisation ΔE_v is related to the free volume, or the concentration of the holes in the liquid determined by the energy of the hole formation.

Four parameters in Equation (1) – the average mass and volume of structural units, the activation energy and the energy of vaporisation – are related to the internal structure of a liquid, or type, concentrations and interactions between structural units at atomic / cation / anion levels. Therefore, their values depend on the definition of a viscous flow structural unit.

A silicate slag structure is conventionally described as the silicate network of SiO_4^{4-} tetrahedra partly disconnected by different metal cations that are distributed to keep the total electro-neutrality [14-15]. A silicate slag may also be considered as a nearly close-packed arrangement of larger oxygen anions with smaller metal cations that occupy the interstices and interact with each other [14]. Fincham and Richardson [16] related properties of a silicate slag to the internal slag structure through concentrations of three different types of oxygens: "bridging" (O^0 – connected to two silicon cations), "non-bridging" (O^- – connected to only one silicon), and "free" (O^{2-} – associated with non-silicon cations). A simplified two-dimensional schematic diagram of the internal structure of slag is shown in **Figure 1**. The viscous flow of the silicate slag in the present model is considered to be the movement of oxygens together with metal cations partly associated with them under the applied shear force, so that the viscous flow structural units are defined as oxygen anions with metal cations partly associated with them, including $Si_{0.5}O$ (= Si-O-Si = Si-Si), $Me^{n+}_{2/n}O$ (= Me-O-Me = Me-Me) and $Me^{n+}_{1/n}Si_{0.25}O$ (= Si-O-Me = Si-Me), where n denotes the oxidation state of a metal cation Me^{n+}. For the binary MeO-SiO_2 silicate slag, three types of structural units can be identified (Si-O-Si) (shaded with dark grey), (Si-O-Me) (shaded with light grey) and (Me-O-Me) (white, not shaded), as indicated in Figure 1. Their molar fractions are expressed as $X_{Si\text{-}Si}$, $X_{Si\text{-}Me}$ and $X_{Me\text{-}Me}$ respectively. Viscous flow structural units differ from the conventional structural units [14-16], however, for simplicity they are referred to just as "structural units".

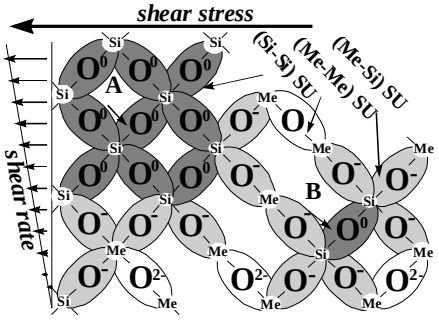

Figure 1 Simplified two-dimensional schematic diagram of internal structure and viscous flow structural units (SU) in silicate melt (O^0, O^-, and O^{2-} correspond to non-bridging, bridging, and free oxygens respectively).

The integral molar activation energy $\overline{E}_a$, the integral molar vaporisation energy $\Delta\overline{E}_V$, and the average molar mass and volume of structural units m_{SU} and v_{SU} in the present model are expressed through mole fractions of the various structural units X_{ij} by following Equation (2):

$$m_{SU} = \sum_{i,j} m_{ij} X_{ij} \; ; v_{SU} = \sum_{i,j} v_{ij} X_{ij} \; ; \; \overline{\boldsymbol{E}}_{\boldsymbol{a}} = \sum_{\boldsymbol{i,j}} \overline{\boldsymbol{E}}_{\boldsymbol{a,ij}} \boldsymbol{X}_{\boldsymbol{ij}} \; ; \Delta \overline{\boldsymbol{E}}_{\boldsymbol{V}} = \Delta \overline{\boldsymbol{E}}_{\boldsymbol{V,0}} \exp\left(\sum_{\boldsymbol{i,j}} \boldsymbol{\varepsilon}_{\boldsymbol{V,ij}} \boldsymbol{X}_{\boldsymbol{ij}} \right) \tag{2}$$

where i and j are metal cations, m_{SU} and v_{SU} are the average molar mass and volume of structural units, m_{ij} and v_{ij} are the masses and volumes of the respective structural unit, $\overline{\boldsymbol{E}}_{\boldsymbol{a,ij}}$ are partial molar activation energies, $\Delta \overline{\boldsymbol{E}}_{\boldsymbol{V,0}}$ is set as 1 J/mol, and $\varepsilon_{V,ij}$ are the dimensionless "partial" vaporisation energy coefficients of the respective structural unit. In the binary MeO-SiO_2 system, these partial activation energies include $\overline{\boldsymbol{E}}_{\boldsymbol{a,Si-Si}}$, $\overline{E}_{a,Si-Me}$ and $\overline{\boldsymbol{E}}_{\boldsymbol{a,Me-Me}}$, and the integral activation energy is expressed as follows:

$$\overline{\boldsymbol{E}}_{\boldsymbol{a}} = \overline{\boldsymbol{E}}_{\boldsymbol{a,Si-Si}} \boldsymbol{X}_{\boldsymbol{Si-Si}} + \overline{\boldsymbol{E}}_{\boldsymbol{a,Si-Me}} \boldsymbol{X}_{\boldsymbol{Si-Me}} + \overline{\boldsymbol{E}}_{\boldsymbol{a,Me-Me}} \boldsymbol{X}_{\boldsymbol{Me-Me}} \tag{2'}$$

The m_{ij} values are molecular weights of the corresponding molecules, such as $Si_{1/2}O$, $Me^{n+}_{2/n}O$ and $Me^{n+}_{1/n}Si_{1/4}O$ respectively. The v_{ij} values are calculated using the effective diameters of structural units estimated from the ionic radii of ions (O, Si, Me) in a particular structural unit; the ionic radii are taken from Shannon [17]. However, the three-dimensional arrangements of the structural units are not taken into account.

In addition to one oxygen, a given structural unit involves two metal cations, both of them have other neighbours and both are involved into other structural unit(s). Therefore, the partial properties $E_{a,ij}$ and $\varepsilon_{V,ij}$ of a given structural unit (i-O-j) depend on the type of neighbours. If the two Si cations in a (Si-O-Si) structural unit have other Me cations as neighbours (for example, see a structural unit marked as "B" in Fig. 1), they will have a different partial activation molar energy compared to the case when some or all other neighbours are also Si cations (for example, see a structural unit marked as "A" in Fig. 1). The effect of neighbouring structural units on a given partial activation energy is expressed as a function of the concentrations of other types of structural units. In the previous model [1-6], the partial molar activation energy of each type of a structural unit in Equation (2) was expressed as the following:

$$\overline{\boldsymbol{E}}_{\boldsymbol{a,Si-Si}} = \boldsymbol{E}^{\boldsymbol{0}}_{\boldsymbol{a,Si-Si}} + \boldsymbol{E}^{\boldsymbol{Si-Si,1}}_{\boldsymbol{a,Si-Si}} \boldsymbol{X}_{\boldsymbol{Si-Si}} + \boldsymbol{E}^{\boldsymbol{Si-Si,2}}_{\boldsymbol{a,Si-Si}} \boldsymbol{X}^{\boldsymbol{2}}_{\boldsymbol{Si-Si}} + \boldsymbol{E}^{\boldsymbol{Si-Me}}_{\boldsymbol{a,Si-Si}} \boldsymbol{X}_{\boldsymbol{Si-Me}} \tag{6}$$

$$\overline{\boldsymbol{E}}_{\boldsymbol{a,Si-Me}} = \boldsymbol{E}^{\boldsymbol{0}}_{\boldsymbol{a,Si-Me}} + \boldsymbol{E}^{\boldsymbol{Si-Me}}_{\boldsymbol{a,Si-Me}} \boldsymbol{X}_{\boldsymbol{Si-Me}} + \boldsymbol{E}^{\boldsymbol{Si-Si}}_{\boldsymbol{a,Si-Me}} \boldsymbol{X}_{\boldsymbol{Si-Si}} + \boldsymbol{E}^{\boldsymbol{Me-Me}}_{\boldsymbol{a,Si-Me}} \boldsymbol{X}_{\boldsymbol{Me-Me}} \tag{7}$$

$$\overline{\boldsymbol{E}}_{\boldsymbol{a,Me-Me}} = \boldsymbol{E}^{\boldsymbol{0}}_{\boldsymbol{a,Me-Me}} + \boldsymbol{E}^{\boldsymbol{Me-Me}}_{\boldsymbol{a,Me-Me}} \boldsymbol{X}_{\boldsymbol{Me-Me}} + \boldsymbol{E}^{\boldsymbol{Si-Me}}_{\boldsymbol{a,Me-Me}} \boldsymbol{X}_{\boldsymbol{Si-Me}} \tag{8}$$

Note that only the effect of the second nearest neighbours was taken into account. For example, $\overline{\boldsymbol{E}}_{\boldsymbol{a,Si-Si}}$ does not depend on $X_{Me\text{-}Me}$, because (Me-O-Me) structural unit cannot be the closest neighbour of the (Si-O-Si) structural unit.

A second power term $\boldsymbol{E}^{\boldsymbol{Si-Si,2}}_{\boldsymbol{a,Si-Si}} \boldsymbol{X}^{\boldsymbol{2}}_{\boldsymbol{Si-Si}}$ was previously introduced [1-6] in the expression of $\overline{\boldsymbol{E}}_{\boldsymbol{a,Si-Si}}$ to describe experimental data in the SiO_2-containing systems. More complex terms in the expression of $\overline{\boldsymbol{E}}_{\boldsymbol{a,Si-Si}}$ were later suggested [7] for the Na- and K-containing silicate slags. The composition dependencies of most other partial activation energies were not taken into account due to their weak dependencies, the lack or uncertainties of

experimental data. The partial activation energies $\overline{E}_{a,Me1-Me2}$ for the slag systems with limited experimental data available (e.g. Al_2O_3-'FeO' and CaO-'FeO') were taken to be equal to ½ ($\overline{E}_{a,Me1-Me1} + \overline{E}_{a,Me2-Me2}$). The dimensionless partial vaporisation energies $\varepsilon_{V,Si-Si}$, $\varepsilon_{V,Si-Me}$ and $\varepsilon_{V,Me-Me}$ were described in a similar way.

However, previous model formalism had some limitations in description of viscosities in complex silicate slag systems, and therefore, in the present study we have revised the quasi-chemical viscosity model formalism. In the revised model, the partial properties $\overline{E}_{a,ij}$ and $\varepsilon_{V,ij}$ of a given structural unit (i-O-j) are described as follows:

$$P_{Si-Si} = P^0_{Si-Si} + \sum_{i=Ca,Mg,Al,...}\left[P^{Si-i}_{Si-Si}\frac{X_{Si-i}}{\left(1-X_{Si-Si}-X_{i-i}\right)^{1-\gamma_{Si/i}}}\right] + \sum_{j=Ca,Mg,...}\left[\Delta P^{Si-Al(T-O,j)}_{Si-Si}\left(X^{ch,j}_{AlO4}X_{Si-Al}\right)^{\gamma_{Si/Al}}\right] \quad (9)$$

$$P_{k-l} \approx P^0_{k-l}, \quad (10)$$

$$P_{Al-m} = P^0_{Al-m} + \sum_{j=Ca,Mg,...}\left(\Delta P^{T-O,j}_{Al-k}X^{ch,j}_{AlO4}\right); \quad X^{ch,j}_{AlO4} = \frac{\left(\sum_n X_{Al-n}\right)^{\alpha_{Al/j}}\left(\sum_n X_{j-n}\right)^{4-\alpha_{Al/j}}}{\left(\sum_n X_{Al-n}+\sum_s\sum_n X_{s-n}\right)^4}\left(\sum_n X_{Al-n}+\sum_n X_{j-n}\right) \quad (11)$$

where: i = *Ca, Mg, Al, Na, …,* j = *Ca, Mg, …(*$j \neq Si, Al$*),* k = *Si, Ca, Mg, Na, …(*$k \neq Al$*),*
l = *Ca, Mg, Na, …(*$l \neq Si, Al$*),* m, n, s = *Si, Ca, Mg, Al,…*

The symbol "*P*" denotes partial properties $\overline{E}_a$ or corresponding ε_V coefficients. In Equation (9), the power coefficient $\gamma_{Si/i}$ is a system-dependent parameter that determines the degree of viscosity decrease with the addition of basic oxides in the silicate melt. $\Delta P^{Si-Al(T-O,j)}_{Si-Si}$ and $\Delta P^{T-O,j}_{Al-i}$ describe additional contribution to the partial molar activation and vaporisation energies of corresponding structural unit due to the presence of tetrahedrally-coordinated Al^{3+}. In Equation (11), the term $X^{ch,l}_{AlO4}$ is related to the probability to have a tetrahedrally-coordinated Al^{3+} involved in the Al-O-Me_j structural units. The power $\alpha_{Al/j}$ determines the proportion of the tetrahedrally-coordinated Al-containing structural units as a result of charge compensation by Me_j cation, and it is determined for the corresponding Al_2O_3-Me_jO oxide binary aluminate system.

The concentrations of structural units in the present study are determined using the quasi-chemical thermodynamic model of the slag developed by Blander and Pelton [18-20] that takes into account the formation of two nearest-neighbour pairs (Si-Me) from a (Me-Me) and a (Si-Si) pair, referred to as "second nearest neighbour bonds" (SNNB) [18-20]. The quasi-chemical thermodynamic model as part of the FactSage computer package [21] has been successfully applied to evaluate phase equilibria and thermodynamic properties in many slag systems, from binary to multi-component systems. The SNNB distributions calculated with the quasi-chemical thermodynamic model were taken as a reasonable approximation of the internal structures of the slags. The important point is that, in constructing the quasi-chemical

thermodynamic model of the liquid slag, valuable information on the liquid slag structure at the atomic level can be obtained. This information can be used as a basis for the description of physicochemical properties. In this study, we assume that the concentrations of the various viscous flow structural units are equal to those of the corresponding second nearest neighbour bonds of the quasi-chemical thermodynamic model. The new thermodynamic database of the system Al-Ca-Fe-K-Mg-Na-O-Pb-Si-Zn [22, 23] has been used to calculate SNNB concentrations.

Present model parameters (partial activation and vaporisation energy coefficients) have physical basis, and they are directly related to the internal slag structure or the physics of interactions at atomic scale. Strong, mostly covalent bonds linking silicate tetrahedrons is attributed to high activation energy and high viscosities in the silica-rich slags. Addition of basic metal oxides strongly affects the formation of the silicate tetrahedrons and therefore has strong effect on the slag properties, e.g. decrease viscosity of the high-silicate slags significantly. Some cations (e.g. Al^{3+}) behave in a different way depending on the chemical environment. The individual effect of various metal oxides on viscosity is determined by atomic structure, cation size, inner and outer electronic arrangements and so on.

The physical basis of the model parameters is a foundation (i) to introduce particular restrictions (e.g. integral activation and vaporisation energies should be positive over the whole composition range), and (ii) to relate these parameters to other known metal cation characteristics (e.g. cation size, ionic potential) or other physicochemical properties (e.g. heat of vaporisation). The optimisation procedures involve active assessments based on accepted experimental data and the use of correlations with other physicochemical properties. The present viscosity model parameters can also help to "de-convolute" relative physicochemical behaviour of different cations in the oxide melt. These considerations were used in the revision of the model formalism and the optimisation of the model parameters.

Systematic optimisation was carried out in cycles from lower order systems to multi-component systems until satisfactory agreement with all accepted experimental data was achieved. **Table 1** reports present model parameters for the Al_2O_3-CaO-MgO-SiO_2 system as an example.

Table 1 Viscosity model parameters for the Al_2O_3-CaO-MgO-SiO_2 system used in the present study

The average mass and volume of structural units.

SU	Si-Si	Al-Al	Ca-Ca	K-K	Mg-Mg	Na-Na	NaAl-NaAl	Si-Al	Si-Ca	Si-K	Si-Mg	Si-Na	Si-NaAl
M,SUx10^{-26}kg	4.99	5.64	9.31	15.64	6.69	10.29	6.81	5.32	7.15	10.32	5.84	7.64	5.90
v,SUx$10^{-29}m^3$	1.92	3.03	5.79	9.00	3.99	5.94	10.38	2.43	3.50	4.58	2.83	3.56	5.01

SU	Al-Ca	Al-K	Al-Mg	Al-Na	Al-NaAl	Ca-K	Ca-Mg	Ca-Na	Ca-NaAl	Mg-K	Mg-Na	Mg-NaAl	Na-K	Na-NaAl
m,SUx10^{-26} kg	7.48	8.79	6.17	7.97	6.23	12.48	8.00	9.80	8.06	11.17	8.49	10.15	12.97	8.55
v,SUx$10^{-29}m^3$	4.27	5.49	3.49	4.32	5.97	7.28	4.84	5.86	7.86	6.16	4.90	6.84	7.47	7.77

Table 1 (continued)

The viscosity activation and vaporisation energy coefficients [J mol^{-1}]. (Al_2O_3-CaO-MgO-SiO_2 system)

$$E_a = E_{a,Si-Si}X_{Si-Si} + E_{a,Si-Al}X_{Si-Al} + E_{a,Si-Ca}X_{Si-Ca} + E_{a,Si-Mg}X_{Si-Mg}$$
$$+ E_{a,Al-Al}X_{Al-Al} + E_{a,Al-Ca}X_{Al-Ca} + E_{a,Al-Mg}X_{Al-Mg} + E_{a,Ca-Ca}X_{Ca-Ca} + E_{a,Ca-Mg}X_{Ca-Mg} + E_{a,Mg-Mg}X_{Mg-Mg};$$

$$E_{a,Si-Si} = 570000 - 407000\frac{X_{Si-Ca}}{(1-X_{Si-Si}-X_{Ca-Ca})^{1-0.32}} - 432000\frac{X_{Si-Mg}}{(1-X_{Si-Si}-X_{Mg-Mg})^{1-0.40}} - 259000\frac{X_{Si-Al}}{(1-X_{Si-Si}-X_{Al-Al})^{1-0.58}}$$
$$+ 3840000\left(X_{AlO4}^{ch,Ca}X_{Si-Al}\right)^{0.58} + 2250000\left(X_{AlO4}^{ch,Mg}X_{Si-Al}\right)^{0.58};$$

$E_{a,Ca-Ca}$ = 78000; $E_{a,Mg-Mg}$ =105000;$E_{a,Si-Ca}$ = 157000; $E_{a,Si-Mg}$ =161000;

$$E_{a,Si-Al} = 187000 + 3780000\,X_{AlO4}^{ch,Ca} + 750000\,X_{AlO4}^{ch,Mg};\quad E_{a,Al-Al} = 169000 + 950000\,X_{AlO4}^{ch,Ca} + 420000\,X_{AlO4}^{ch,Mg};$$
$$E_{a,Al-Ca} = 122000 + 705000\,X_{AlO4}^{ch,Ca} + 2000000\,X_{AlO4}^{ch,Mg};\quad E_{a,Al-Mg} = 140000 + 2000000\,X_{AlO4}^{ch,Ca} + 400000\,X_{AlO4}^{ch,Mg};$$

the rest $E_{a,i\text{-}j}$, = 1/2 ($E_{a,i\text{-}i}$ + $E_{a,j\text{-}j}$)

$$\Delta E_V = \exp(\varepsilon_{V,Si-Si}X_{Si-Si} + \varepsilon_{V,Si-Al}X_{Si-Al} + \varepsilon_{V,Si-Ca}X_{Si-Ca} + \varepsilon_{V,Si-Mg}X_{Si-Mg}$$
$$+ \varepsilon_{V,Al-Al}X_{Al-Al} + \varepsilon_{V,Al-Ca}X_{Al-Ca} + \varepsilon_{V,Al-Mg}X_{Al-Mg} + \varepsilon_{V,Ca-Ca}X_{Ca-Ca} + \varepsilon_{V,Ca-Mg}X_{Ca-Mg} + \varepsilon_{V,Mg-Mg}X_{Mg-Mg});$$

$$\varepsilon_{V,Si-Si} = 23.6 - 7.6\frac{X_{Si-Ca}}{(1-X_{Si-Si}-X_{Ca-Ca})^{1-0.32}} - 8.7\frac{X_{Si-Mg}}{(1-X_{Si-Si}-X_{Mg-Mg})^{1-0.40}} - 0.0\frac{X_{Si-Al}}{(1-X_{Si-Si}-X_{Al-Al})^{1-0.58}}$$
$$+ 195\left(X_{AlO4}^{ch,Ca}X_{Si-Al}\right)^{0.58} + 85\left(X_{AlO4}^{ch,Mg}X_{Si-Al}\right)^{0.58};$$

$\varepsilon_{V,Ca\text{-}Ca}$ =13.5; $\varepsilon_{V,Mg\text{-}Mg}$ =14.1; $\varepsilon_{V,Si\text{-}Ca}$ =15.7; $\varepsilon_{V,Si\text{-}Mg}$ =15.8;

$$\varepsilon_{V,Si-Al} = 16.3 + 216\,X_{AlO4}^{ch,Ca} + 50\,X_{AlO4}^{ch,Mg};\quad \varepsilon_{V,Al-Al} = 15.5 + 42\,X_{AlO4}^{ch,Ca} + 22\,X_{AlO4}^{ch,Mg};$$
$$\varepsilon_{V,Al-Ca} = 14.0 + 36\,X_{AlO4}^{ch,Ca} + 0.0\,X_{AlO4}^{ch,Mg};\quad \varepsilon_{V,Al-Mg} = 14.8 + 0.0\,X_{AlO4}^{ch,Ca} + 20\,X_{AlO4}^{ch,Mg};$$

the rest ε_V; $\varepsilon_{V,i\text{-}j} = 1/2\left(\varepsilon_{V,i\text{-}i} + \varepsilon_{V,j\text{-}j}\right)$

3. Results and Discussion

3.1 Pure oxide properties

First, activation and vaporisation energies of pure SiO_2, Al_2O_3 and PbO melts have been determined using available experimental data. The calculated and experimental viscosities of pure oxide melts are shown in **Figure 2,** and it demonstrates good agreement. The activation and vaporisation energies for pure CaO, MgO, Na_2O and K_2O melts were derived from experimental data in the corresponding binary silicate systems, as well as trend analyses the model parameters related to available structural and other physicochemical properties, as described in the following.

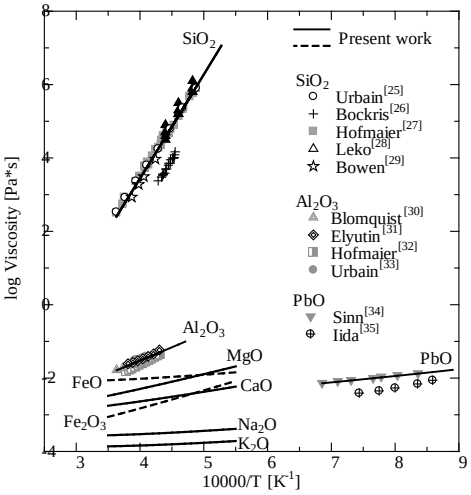

Figure 2 Calculated viscosities of pure oxide melts as functions of temperature. Results for 'FeO' and Fe_2O_3 were obtained from reference [36].

Figure 3 (a) shows the relationship between the activation energies for pure oxides and the ionic potentials of the corresponding cations, which is defined as the ratio of the valence to the radius of a cation. The activation energy is higher for the cations with higher ionic potentials, indicating that the cation has stronger bonds with oxygen anions. **Figure 3 (b)** shows the relationship between the vaporisation energies for pure oxides and the enthalpies of decomposing liquid oxides into elemental gas species, calculated with the latest thermodynamic databases

in the FactSage computation package [21-24] on the basis of the following reaction: $Me_{2/n}O$ (Liquid) = 2/*n* Me(Gas) + O (Gas), where *n* denotes the oxidation state of a cation. **Fig. 3 (b)** indicates that the vaporisation energy for pure SiO_2 is much higher than the others, and no particular trend was indicated for other metal oxides. Significantly higher activation and vaporisation energy, and viscosity of pure SiO_2 than other oxide melts may be attributed to the strong covalent bonds between silicon cations and oxygen anions. Note that the values of the parameters for SiO_2, Al_2O_3 and PbO (described by squares) coincide with experimental points available for the corresponding pure oxides; those for the others (described by circles) have no experimental points for comparisons, and were obtained by fitting the predictions into experimental data in the composition areas close to the corresponding oxides in binary and higher order systems.

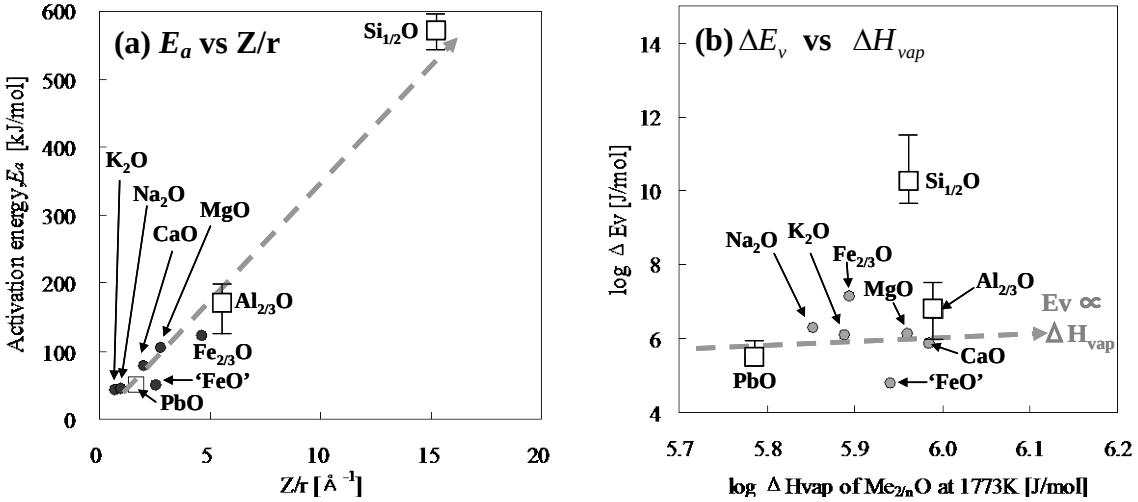

Figure 3 (a) Correlation between the activation energy of pure oxide melt and ionic potential for the corresponding cation. (b) Correlation between the vaporisation energy for pure oxide melt and the enthalpy of decomposing oxide component into elemental gas species, calculated using the FactSage thermodynamic computation program. Data for 'FeO' and $Fe_{2/3}O$ were from reference [36].

3.2 Binary and ternary silicate systems

Figure 4 shows the fractions of the Si-Si, Si-Me and Me-Me structural units in various $Si_{1/2}O$-$Me_{2/n}O$ systems, obtained from the quasi-chemical thermodynamic model [18-20]. The ordering as the preference to form Si-Me over Me-Me and Si-Si SNNB decreases from the Na_2O-, K_2O- and CaO- to MgO-, PbO-, 'FeO'- and Al_2O_3-silicate system. It should be emphasized that the Si-Me and Si-Si structural units are predominant and determine the viscosity in the melt at high SiO_2 contents. This internal structural information is essential for understanding of the detailed trends in the developed model, and was therefore used in the optimisation of model parameters for binary silicate systems.

Figure 5 shows the calculated and experimental slag viscosities of several binary silicate systems, indicating that the addition of basic metal oxides into silica-rich slag significantly (by orders of magnitude) decreases viscosity. This significant viscosity decrease is generally attributed to the disturbance of the strong covalent bonds in the silicate tetrahedral network structures by metal cations. Therefore, the degree of this viscosity decrease could be related to cation size, valence, inner and outer electronic arrangement, and the "ease" for cations to donate valent electrons to the oxygen anions in the melt. It follows that the degree of viscosity decrease should be specific for a given metal oxide.

A use of a second power term $E_{a,Si-Si}^{Si-Si,2} X_{Si-Si}^{2}$ in the previous QCV model [1-7] resulted in systematic discrepancies: predicted viscosities were commonly higher than experimental data at high SiO_2 concentrations. The revised model (see Equation (9)) has the Si-Si partial activation and vaporisation energies in different SiO_2-MeO systems expressed by a power function of the concentrations of the Si-Me structural units. In a binary silicate system, Equation (9) reduces to the following Equation (12):

$$E_{a,Si-Si} = E_{a,Si-Si}^{0} + E_{a,Si-Si}^{Si-Me} X_{Si-Me}^{\gamma_{Si/Me}}; \quad \varepsilon_{V,Si-Si} = \varepsilon_{V,Si-Si}^{0} + \varepsilon_{V,Si-Si}^{Si-Me} X_{Si-Me}^{\gamma_{Si/Me}} \tag{12}$$

where the parameters $E_{a,Si-Si}^{Si-Me}$ and $\varepsilon_{V,Si-Si}^{Si-Me}$ (both having negative values) describe the degree of viscosity decrease with increasing the Si-Me structural unit concentrations as a result of complex interactions in the silicate melt; and the power parameter $\gamma_{Si/Me}$ may be related to the effective number of the Si-Si structural units which are affected by one given Si-Me structural unit. All these parameters depend on how basic the metal cation Me^{n+} behaviour is in affecting the strength of the predominantly covalently-bonded silicate tetrahedral structures, and therefore are expected to correlate with the ionic potential (see the relationships in **Figure 7**).

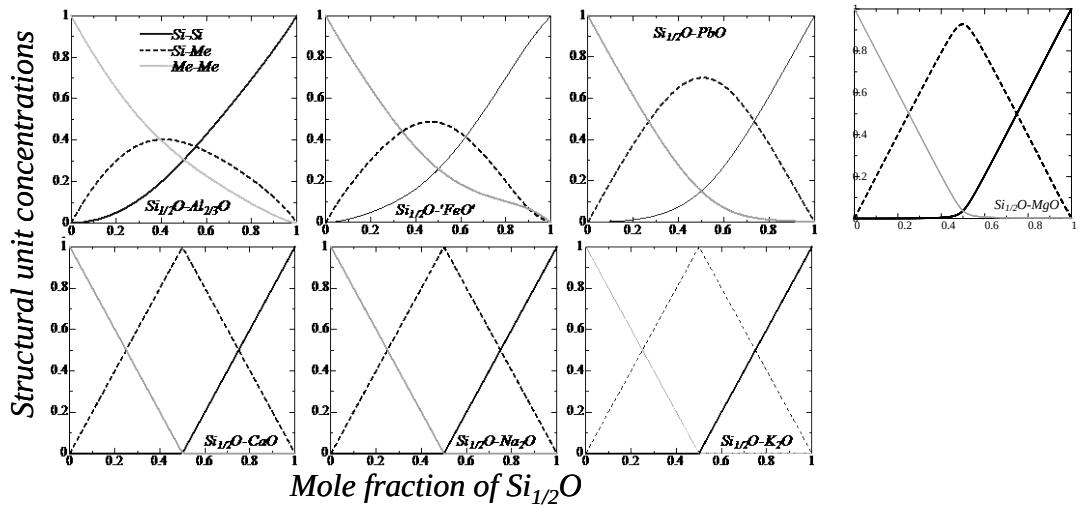

Figure 4 The concentrations of the structural units in the $Si_{1/2}O$-$Me_{2/n}O$ systems (Me = Al, Fe^{2+}, Pb, Mg, Ca, Na, K, *n*: ionic valence of the Me^{n+} cation).

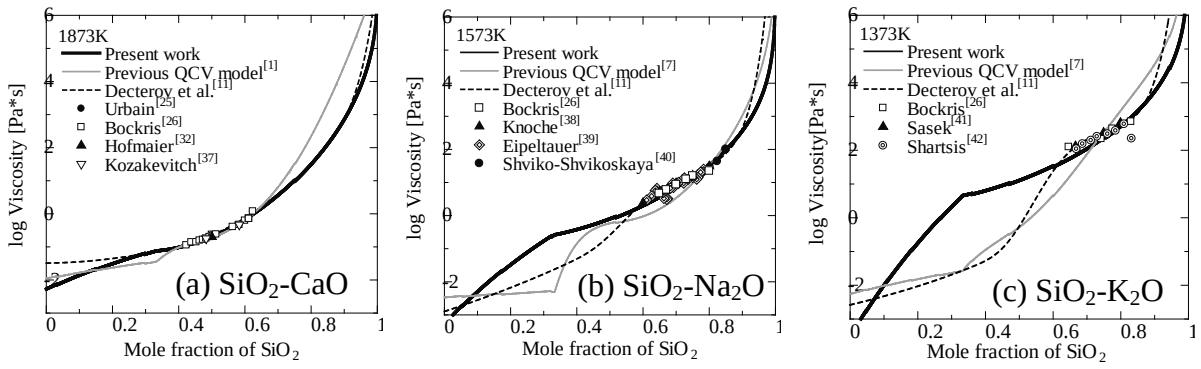

Figure 5 Calculated viscosities of fully liquid slag for binary silicate systems: (a) SiO_2-CaO at 1873 K, (b) SiO_2-Na_2O at 1573 K, (c) SiO_2-K_2O at 1373 K.

Fig. 7 (a) indicates that the inversed value of the power parameter $\gamma_{Si/Me}$ linearly increases with the ratio of ionic potentials I_{Si} / I_{Me}. The trend in **Fig. 7 (b)** is not clear, but may be taken to indicate that the activation energy coefficient $E_{a,Si-Si}^{Si-Me}$ tends to decrease with increasing the ratio of ionic potentials I_{Si} / I_{Me} Therefore, it may be argued that, a Me^{n+} cation with larger size and lower ionic potential has the ability to affect more surrounding Si-Si structural units and to reduce their partial activation energies more significantly, which is expressed by lower $\gamma_{Si/Me}$ and $E_{a,Si-Si}^{Si-Me}$ values. This tendency corresponds to significant decrease of the viscosity of the SiO_2-MeO silicate melt with addition of the basic oxide. **Figure 8** demonstrates that for a number of binary silicate systems the activation energy at high SiO_2 concentrations shows significant decrease with the $\gamma_{Si/Me}$ decrease.

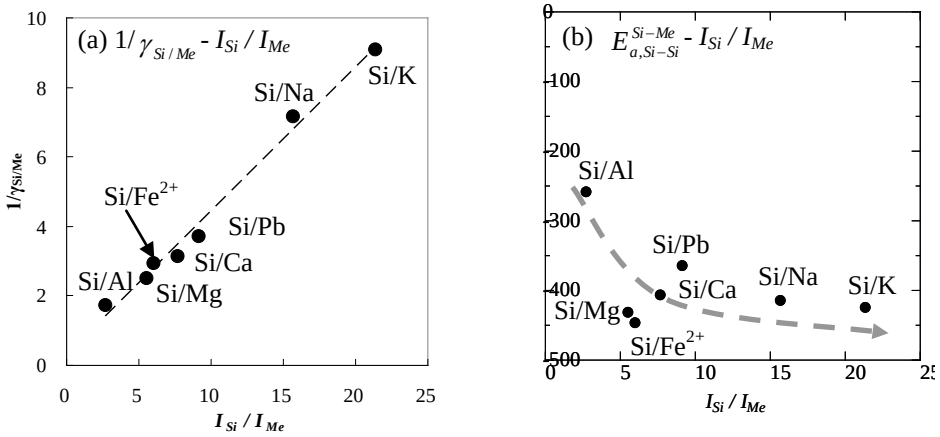

Figure 7 Correlations between the activation energy coefficients for binary silicate systems and the ratio of ionic potential*:* (a) $1/\gamma_{Si/Me}$ - I_{Si} / I_{Me}**,** (b) $E_{a,Si-Si}^{Si-Me}$ - I_{Si} / I_{Me}**.** Data for the SiO_2-'FeO' system is from reference [36].

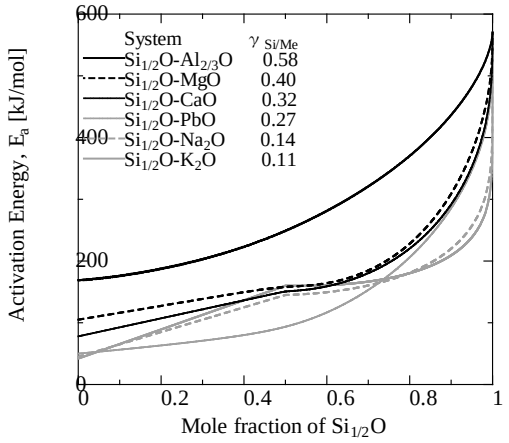

Figure 8. Calculated integral activation energies for the $Si_{1/2}O$-$Me_{2/n}O$ systems. (Me = K, Na, Pb, Ca, Mg, Al, *n*: ionic valence of the Me^{n+} cation).

In relation to the ternary silicate systems SiO_2-Me1O-Me2O, it has been assumed that the partial and integral activation and vaporisation energies vary as follows: (i) along the constant ratio of two metal oxides - as a function of SiO_2 concentrations is similar change to those in the binary silicate systems, and (ii) along the constant SiO_2 concentrations - as a function of the basic metal oxide ratios is close to the linear relationship. To describe these trends, the model formalism for binary silicate systems described in Equation (12) has been extrapolated into ternary and multi-component systems as shown in Equation (9). **Figure 9** shows the viscosities in the SiO_2-CaO-MgO system at a

fixed SiO_2 content, indicating linear change with the MgO/(CaO+MgO) molar ratio. Note that the calculated results outside the liquidus are extrapolations that may be taken as those in metastable liquid.

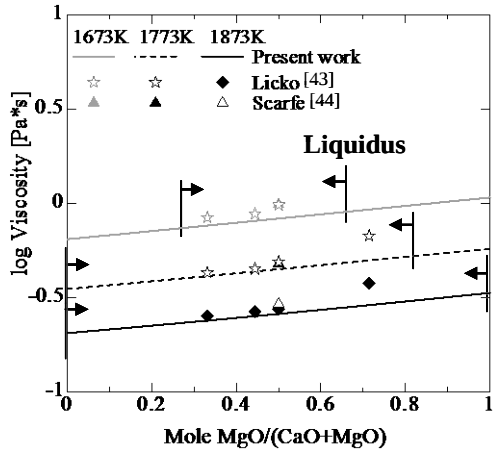

Figure 9 Comparison between calculated and experimental slag viscosities in the SiO_2-CaO-MgO system, where SiO_2 molar content is kept as 50 mol%.

3.3 Charge compensation effect in Al_2O_3-containing systems

Experimental results indicate that the viscosities in the Al_2O_3-containing silicate systems Al_2O_3-(Me^+, Me^{2+})$_x$O-SiO_2 exhibit maxima at intermediate (Me^+,Me^{2+})O/Al_2O_3 ratios (for example, in the systems Al_2O_3-CaO-SiO_2 [25, 37, 45], Al_2O_3-MgO-SiO_2 [45], and Al_2O_3-Na_2O-SiO_2 [46-47]). This viscosity maximum is attributed to the so-called "charge compensation effect" explained as the Al^{3+} cation's ability to take the tetrahedral interstitial between the oxygen anions if the excess negative charge for Al^{3+} is compensated by the alkali or alkaline earth cations.

In the initial QCV model [1-6], a special charge compensation term was added to the activation energy of viscous flow, which is based on the assumption [48] that the charge compensation effect appears when the Al^{3+} replaces Si^{4+} in the tetrahedral coordination, thus keeping the silicate network structure instead of breaking it. This mechanism related the charge compensation effect to the presence of the silicate networks, and therefore, the charge compensation term was assumed as proportional to the Si-Si structural unit concentration. However, that description had subsequently been revised [7], because (i) it assumed a long-range (further than the second nearest neighbour) interactions, and (ii) it did not reflect the fact that viscosity maximum was observed also in the SiO_2-free systems (e.g. CaO-Al_2O_3 [49]). It should be noted that the strength of the individual (Si-O-Si) bonds is independent of the formation of the tetrahedral Al^{3+} at a distant atomic position. The increase of viscosity associated to the charge compensation effect is assumed to be due to (i) strong (Al-O-Al) or (Al-O-Si) bonds involving tetrahedral Al^{3+} and (ii) lower effect of Al^{3+} cations on the predominantly covalently-bonded Si-Si structural unit because a proportion of Al^{3+} is not in octahedral but in tetrahedral coordination. These effects do not necessarily depend on the presence of Si-Si structural unit, which agree with experimental evidence [49].

In the present model, a parameter related to the proportion of the tetrahedral Al^{3+}, $X_{AlO_4}^{ch,j}$ is introduced, and its additional contribution to the activation and vaporisation energies of the Al_2O_3-containing structural units is assumed as proportional to this $X_{AlO_4}^{ch,j}$ value. Moreover, the weakening of the effect of Al^{3+} cations on decreasing the partial molar energies of the Si-Si structural units is described by additional term to the partial energies of Si-Si structural unit, which has positive coefficients and is proportional to the effective fraction of the tetrahedral Si-Al structural units

counted as affecting one Si-Si structural unit. The above improvements are described in Equations (9-11). Unlike the Ca-, Fe- and Mg-containing aluminate systems, the charge compensation effect in the Na-containing aluminate systems is described in the latest quasi-chemical thermodynamic model by the formation of $NaAlO_2$ associates [23, 44], and in the present viscosity model by the activation and vaporisation energies expressions without the above special adjustments.

Figure 10 shows the comparison of the viscosities at 50 mol% SiO_2 for various ternary aluminosilicate melts. The predicted viscosities show upward curvatures due to the contribution of tetrahedral Al^{3+} coordination, and they agree with experimental data. It was indicated that the viscosity maximum decreases in the series of (Na-Al-Si-O) > (Ca-Al-Si-O) > (Mg-Al-Si-O) > (Fe^{2+}-Al-Si-O) systems.

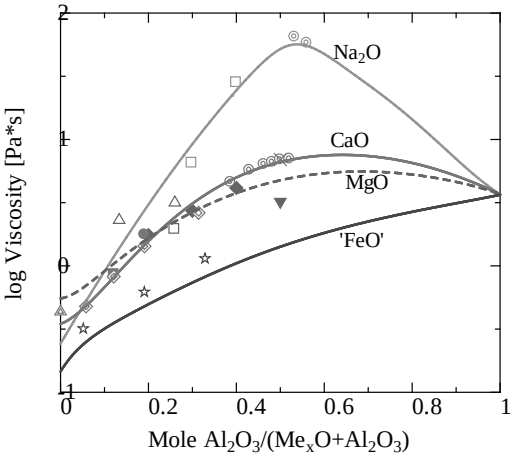

Figure 10 Calculated viscosities of the Al-Me-O-Si melts at 1773 K (Me = Na, Ca, Mg, Fe^{2+}) at 50 mol% SiO_2. Result for the Al-Fe^{2+}-O-Si system was from reference [36].

3.4 Application of the present viscosity model to multi-component oxide systems

The revised QCV model formalism has been successfully extended to multi-component oxide systems, and slag viscosities have been evaluated with the same set of model parameters as used for binary and ternary systems. The accuracies of the calculated viscosities were evaluated with the average of the relative errors derived by the following:

$$\text{Average of relative errors (\%)} = \frac{100}{N}\sum_{i=1}^{N}\left|\frac{\eta_{Calc,i}-\eta_{Expe,i}}{\eta_{Expe,i}}\right| \qquad (13)$$

where *N* denotes total number of accepted experimental data. **Figure 11** summarizes the average of relative errors for various subsystems included in the multi-component system SiO_2 - Al_2O_3 - CaO - MgO - Na_2O - K_2O - 'FeO' - Fe_2O_3 - PbO - ZnO equilibrated with metallic iron. The calculated viscosities using the revised QCV model and the viscosity model by Decterov *et al.* [8] were used to compare with over 7000 experimental data. It has been found that these experimental data are reproduced by the revised QCV model within 25 % as the average of the relative errors.

In addition, viscous behaviour of molten slag has been predicted using the revised QCV model for the composition range of interest to metallurgical processes where no experimental results are available. **Figure 12** shows the predicted iso-viscosity contours of Al_2O_3-CaO-MgO-15 mass% SiO_2 system, which can include ladle slag compositions formed in BOF or EAF process in iron and steelmaking. It is indicated that slag viscosities at high Al_2O_3 mass fractions have maxima in the middle of MgO / CaO mass ratio due to the maximum contribution of the formation of tetrahedrally-coordinated Al^{3+} to slag viscosities.

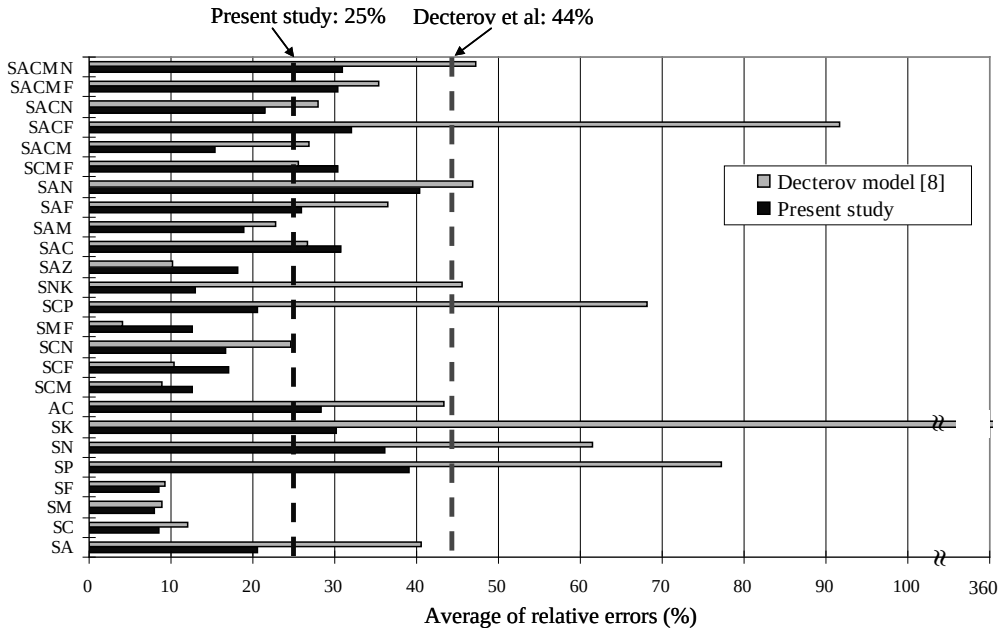

Figure 11 Average of relative errors between calculated viscosities and experimental data for oxide subsystems included in the SiO_2 - Al_2O_3 - CaO - MgO - Na_2O - K_2O - 'FeO' - Fe_2O_3 - PbO - ZnO system equilibrated with metallic iron. (S = SiO_2, A = Al_2O_3, C = CaO, M = MgO, N = Na_2O, K = K_2O, F = 'FeO' or Fe_2O_3, P = PbO, Z = ZnO)

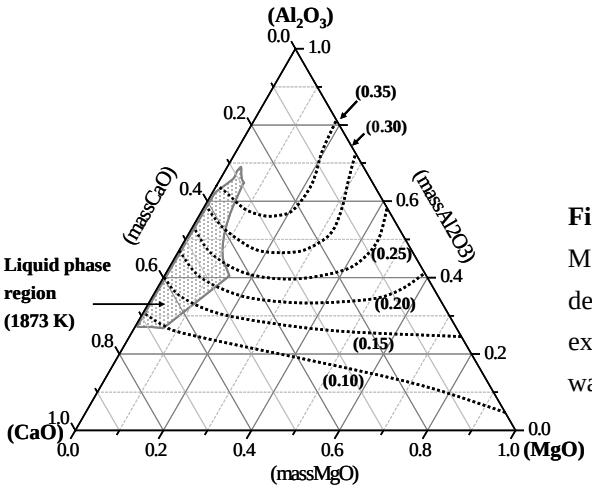

Figure 12 Predicted iso-viscosity contours in the Al_2O_3 - CaO - MgO - 15 mass% SiO_2 system at 1873 K. Viscosities are described in Pa*s. The sum of mass fractions of all components except SiO_2 has been converted into unity. Liquid phase region was obtained from the FactSage computation package [21].

4. Conclusions

The quasi-chemical viscosity model has been revised that makes it possible to predict the viscosities of fully liquid multi-component silicate slags over wide composition and temperature ranges on the basis of physicochemical characteristics of the oxide melts. Agreements with available experimental viscosity data has been improved from the previous model, and the accuracies are enough high to reproduce viscosity data within experimental uncertainties.

Some important relationships have been found between model parameters and other physicochemical properties of oxide components, such as ionic potentials and heat of vaporisation. These correlations have significantly assisted to determine model parameters for the systems where few experimental data are available.

Acknowledgements

The authors are grateful to Prof. Peter Hayes for useful critical suggestions on model development, support and review of the paper. The authors acknowledge the financial support from the Australian Research Council (ARC) Linkage program for this research to be carried out.

References

[1] A. Kondratiev, E. Jak. A quasi-chemical viscosity model for fully liquid slags in the Al_2O_3-CaO-'FeO'-SiO_2 system, *Metall. Mater. Trans. B*, 2005, vol.36B, p623-638.

[2] A. Kondratiev, P. C. Hayes, E. Jak. Development and application of a quasi-chemical viscosity model for Al_2O_3-CaO-"FeO"-MgO-SiO_2 slags, *150th ISIJ Meeting*, Hiroshima, Japan, 2005, CAMP-ISIJ, vol.18(4), p 821-825.

[3] A. Kondratiev, P. C. Hayes, E. Jak. Development of a quasi-chemical viscosity model for fully liquid slags in the Al_2O_3-CaO-'FeO'-MgO-SiO_2 system. Part 1. Description of the model and its application to the MgO, MgO-SiO_2, Al_2O_3-MgO and CaO-MgO sub-systems, *ISIJ Int.*, 2006, vol.46(3), p359-367.

[4] A. Kondratiev, P. C. Hayes, E. Jak. Development of a quasi-chemical viscosity model for fully liquid slags in the Al_2O_3-CaO-'FeO'-MgO-SiO_2 system. Part 2. A review of the experimental data and the model predictions for the Al_2O_3-CaO-MgO, CaO-MgO-SiO_2 and Al_2O_3-MgO-SiO_2 systems, *ISIJ Int*., 2006, vol.46(3), p368-374.

[5] A. Kondratiev, P. C. Hayes, E. Jak. Development of a quasi-chemical viscosity model for fully liquid slags in the Al_2O_3-CaO-'FeO'-MgO-SiO_2 system. Part 3. Summary of the model predictions for the Al_2O_3-CaO-MgO-SiO_2 system and its sub-systems, *ISIJ Int.*, 2006, vol.46(3), p375-384.

[6] A. Kondratiev, P. C. Hayes, E. Jak. Development of a quasi-chemical viscosity model for fully liquid slags in the Al_2O_3-CaO-'FeO'-MgO-SiO_2 system. Part 4. The experimental data for the 'FeO'-MgO-SiO_2, CaO-'FeO'-MgO-SiO_2 and Al_2O_3-CaO-'FeO'-MgO-SiO_2 systems at iron saturation, *ISIJ Int.*, 2008, vol.48(1), p7-16.

[7] E. Jak. Viscosity model for slags in the Al_2O_3-CaO-'FeO'-K_2O-Na_2O-MgO-SiO_2 system, *Proc. 8th Int. Conf. Molten Slags Fluxes Salts*, 2009, Santiago, Chile, p433-448.

[8] A. N. Grundy, H. Liu, I-H Jung, S. A, Decterov, A. D. Pelton. A model to calculate the viscosity of silicate melts part I: viscosity of binary SiO_2-MeO_x systems (Me = Na, K, Ca, Mg, Al), *Int. J. Mat. Res*., 2008, vol.99(11),p1185-1194.

[9] A. N. Grundy, H. Liu, I-H Jung, S. A, Decterov, A. D. Pelton. A model to calculate the viscosity of silicate melts part II: The $NaO_{0.5}$-MgO-CaO-$AlO_{1.5}$-SiO_2 system, *Int. J. Mat. Res*., 2008, vol.99(11),p1195-1204.

[10] L. Zhang, S. Jahanshahi. *Metall. Mater. Trans. B*, 1998, vol.29B, p177-186. ibid. p187-195.

[11] M. Nakamoto., J. Lee, T. Tanaka. *ISIJ Int.*, 2003, vol.45(5), p651-656.

[12] J. Frenkel. *Z. Phys.*, 1926, vol.35, p652-669. J. Frenkel. *Trans. Faraday Soc.*, 1937, vol.33, p58-65. J. Frenkel. *Kinetic Theory of Liquids*, Oxford University Press, UK, 1946.

[13] H. Eyring. *J. Chem. Phys.*, 1936, vol.4, p283-291. R. Ewell, H. Eyring. *J. Chem. Phys*., 1937, vol.5, p726-736. S. Glasstone, K. J. Laidler, H. Eyring. *Theory of the Rate Processes*, McGraw-Hill, NY, 1941.

[14] W. D. Kingery, H. K Bowen, D. R. Uhlmann. *Introduction to Ceramics*, John Wiley & Sons, Toronto, 1976.

[15] Y. Waseda, J. M. Toguri. *The Structure and Properties of Oxide Melts*, World Scientific, Singapore, 1998.

[16] J. B. Fincham, F. D. Richardson. *Proc. Royal Soc. (London)*, 1954, vol.223, p40-62.

[17] R. D. Shannon. *Acta Crystallographica*, 1976, vol.A32, p751-767.

[18] M. Blander, A. D. Pelton. *2nd Int. Symp. Metall. Slags Fluxes*, 1984, TMS-AIME, Warrendale, PA, p295-304.

[19] A. D. Pelton, S. A. Decterov, G. Eriksson., C. Robelin, Y. Dessureault. The modified quasichemical model. I-binary

solutions, *Metall. Mater. Trans. B*, 2000, vol.31B. p651–659.

[20] A. D. Pelton, P. Chartrand. The modified quasichemical model. II—multicomponent solutions, *Metall. Mater. Trans. A*, 2001, vol. 32A. p1355-1360.

[21] FactSage, 2012, Ecole Polytechnique, Montréal, http://www.factsage.com/.

[22] S. A. Decterov, I-H Jung, E. Jak, Y. B. Kang, P. C. Hayes, A. D. Pelton. *7th Int Conf Molten Slags Fluxes Salts*, 2004, Cape Town, South Africa, publ. SAIMM, Johannesburg, SA, p839-850.

[23] E. Jak, P. C. Hayes. Final report, "Prediction of liquidus temperatures and high temperature phase equilibria for the system SiO_2-Al_2O_3-FeO-Fe_2O_3-CaO with addition of Na_2O-K_2O-MgO", 2004, The Univerisity of Queensland, Centre for Coal in Sustainable Development (CCSD), Brisbane, Australia, www.ccsd.biz.

[24] ChemApp, 2012, GTT Technologies, Germany, http://www.gtt-technologies.de/.

[25] G. Urbain, Y. Bottinga, P. Richet. *Geochim. Cosmochim. Acta*, 1982, vol.46, p1061-1072.

[26] J. O'M Bockris, J. D. MacKenzie, J. A. Kitchener. Viscous flow in silica and binary liquid silicates, *Trans. Faraday Soc.*., 1955, vol.51, p1734-1748.

[27] G. Hofmaier, G. Urbain. *Science of Ceramics*, 1968, vol.4, p25-32.

[28] V. K. Leko, E. V. Meshcheryakova, N. K. Gusakova, R. B. Lebedeva. *Sov. J. Opt. Technol.*, 1974, vol.41,p600-603.

[29] D. W. Bowen, R. W. Taylor, *Ceram. Bull.*, 1978, vol.57, p818-819.

[30] R. A. Blomquest, J. K. Fink, L. Leibowitz. *Ceram.Bull.*, 1978, vol.57, p522.

[31] V. P. Elyutin, B. C. Mitin, Y. A. Nagibin. *Fiz.Aerodispersnykh Sist.*, 1972, vol.7, p129-135.

[32] G. Hofmaier. *Berg und Huttenm. Monatsh. Montan. Hochschule Loeben*, 1968, vol.113, p270-281.

[33] G. Urbain. *Rev. Int. Haut. Temp. Refract.*, 1983, vol.20, p135-139.

[34] E. Sinn. *Kristall und Technik.*, 1979, vol.14, p117-127.

[35] T. Iida, Z. Morita, T. Rokutanda. *3rd Int. Conf. Molten Slags Fluxes*, 1989, Glasgow, UK, p195-198.

[36] E. Jak, M. Suzuki, M. Chen. Private communications, 2011.

[37] P. Kozakevitch. *Rev. Metall*., 1960, vol.57, p149-160.

[38] R. Knoche, D. B. Dingwell, F. A. Seifert, S. L. Webb. Non-linear properties of supercooled liquids in the system Na_2O-SiO_2, *Chemical geology.*, 1994, vol.116, p1-16.

[39] E. Eipeltauer, G. Jangg. Über die Beziehung zwischen Viskosität und Zusammensetzung binärer Natriumsilikatgläser I., *Kolloid Zeitschrift und Zeitschrift fur Polymere*, 1955, vol.142, p77-84.

[40] T. P. Shvaiko-Shvaikovskaya, O. V. Mazurin, Z. S. Bashun. Viscosity of sodium oxide-silicon dioxide system glasses in molten state., *Izvestiya Akademii Nauk SSSR. Neorganicheskiye Materialy*, 1971, vol.7(1), p143-147.

[41] L. Sasek. The viscosity of silicate glass melts., *Silikaty*, 1977, vol.21, p291-305.

[42] L. Shartsis, S. Spinner, W. Capps. Density, expansivity, and viscosity of molten alkali silicates., *J. Am. Ceram. Soc.*, 1952, vol.35, p155-160.

[43] T. Licko, V. Danek. *Phys. Chem. Glasses*, 1986, vol.27, p22-26.

[44] C. M. Scarfe, D. J. Cronin. *Am. Mineral.*, 1986, vol.71, p767-771.

[45] M. J. Toplis, D. B. Dingwell. Shear viscosities of CaO-Al_2O_3-SiO_2 and MgO-Al_2O_3-SiO_2 liquids: Implications for the structural role of aluminium and the degree of polymerisation of synthetic and natural aluminosilicate melts, *Geochim. Cosmochim. Acta.*, 2004, vol.68, p5169-5188

[46] M. J. Toplis, D. B. Dingwell, T. Lenci. Peraluminous viscosity maxima in Na_2O-Al_2O_3-SiO_2 liquids: The Role of Triclusters in Tectosilicate Melts, *Geochimica et Cosmochimica Acta*, 1997, vol.61, p2605-2612.

[47] E. F. Riebling. Structure of sodium aluminosilicate melts containing at least 50 mole % SiO_2 at 1500C, *J. Chem. Phys.*, 1966, vol.44, p2857-2865.

[48] B. O. Mysen. *Dev. Geochem.*, 1988, vol.4, p1-354.

[49] G. Urbain. *Rev. Int. Haut. Temp. Refract*., 1983, vol.20, p135-139.